sLHC Project Note 0006

2009-11-02

jim@stovall.net

Quadrupole Law and Steering Options in the Linac4 DTL

J. Stovall / BE-ABP, K. Crandall / Crandall Consults.

Keywords: Linac4, drift tube, DTL,

Summary

The Linac4 drift-tube linac (DTL) reference design has been modified to reduce the power consumption in tank 1 by adjusting the accelerating field and phase laws. In this note we investigate three options for the transverse focusing lattice, quadrupole law, and two options for beam steering. We use acceptance, sensitivity to alignment errors and the probabiity of beam loss as figures of merit for evaluating each option.

1. Introduction

The Linac4 drift-tube linac (DTL) reference design has been modified to reduce the power consumption in tank 1 by adjusting the accelerating field and phase law. It is characterized by a slightly higher accelerating field and a more shallow phase ramp beginning at φ_s=-35° in tank 1 as shown in figures 1 and 2. In this note we investigate three options for the transverse focusing lattice and two options for beam steering. We use acceptance, sensitivity to alignment errors and the probabiity of beam loss as figures of merit for evaluating each option.

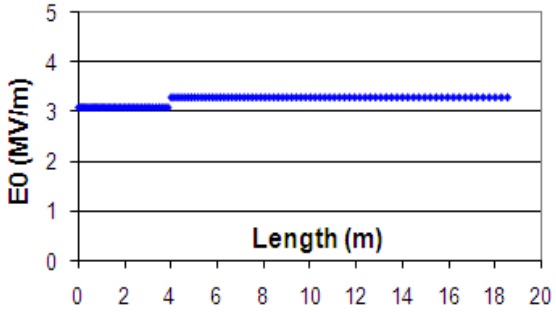

Figure 1. Rev.01 Accelerating field.

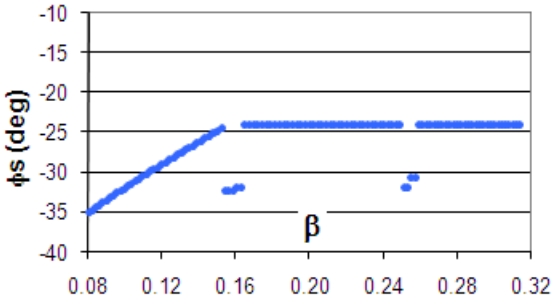

Figure 2. Rev.01 Phase law.

2. Quadrupole law options

We have looked into the following 5 lattice options to provide transverse focusing:

1. FDFD. This 2-cell period lattice is the default design. It requires the highest magnetic gradients (≤100 T/m) and a full compliment (117) of permanent magnet quadrupoles, PMQs. Because of the number and strengths of the lenses, we will show that this lattice is the most sensitive to alignment errors.

2. F0D0. This lattice, having a 4-cell period, requires only half the number of PMQs at strengths about 75% of the FDFD lattice values. These two features reduce its sensitivity to alignment errors. We can arrange to make the "0" quadrupole occur in the inter-tank space giving us more room for diagnostics and steering.

3. FFDD. The beam in this lattice, also having a 4-cell period, is slightly larger, but the quadrupole gradients are only about 50% of the FDFD values and is the least sensitive to alignment errors. In this lattice the beam is nominally parallel between lenses of the same sign. As a result, if we start the lattice at the correct point in the period, we can arrange for the beam to be nominally parallel as it enters the first inter-tank gap. In this case we can omit the inter-tank quadrupole between tanks 1 and 2 without significantly disrupting the periodicity of the beam, giving us more room for diagnostics and steering.

4. FF0DD0. The SNS DTL uses this lattice, having a 6-cell period, for several reasons. Some of the empty drift tubes contain beam position and phase monitors (BPMs) while others contain steering magnets. This offers a great amount of flexibility for steering and rf tuning. This lattice, having a long period, was also more compatible with both the MEBT and CCL which precede and follow the DTL. Unlike SNS, Linac4 has a flat E_0 which makes the longitudinal focusing forces very strong in the beginning of tank 1 with σ_{0l} approaching 90°/period. To meet the other DTL design requirements the transverse focusing forces required, using this lattice, would have to be even stronger, with σ_{0t} exceeding 90°/period, which would risk exciting a parametric resonance.

5. FFFDDD. This 6-cell lattice is rarely used and is incompatible with Lnac-4 for the same reason described above.

The quadrupole gradients for each of the first three lattices were selected to comply with the following design guidelines.

1. $\sigma_{0t} \leq$ 90 °/period
2. $\sigma_{0t} \neq n\sigma_{0l}/2$, for n=1,3,…
3. equipartitioning ratio ≈1.0 at full current
4. dynamics to avoid known parametric resonances

Figure 3 shows the quadrupole gradients required to meet these constraints for the first three lattice options.

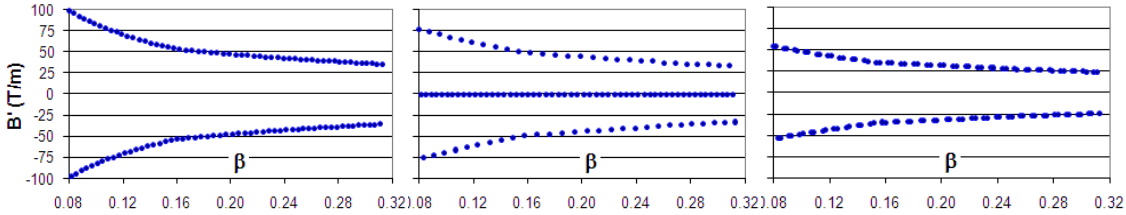

Figure 3. Quadrupole law options, a. FDFD, b. F0D0, c. FFDD.

Figure 4 shows the transverse and longitudinal real-estate phase advance, k_t and k_l, for the FFDD lattice design at the full design current of 64 mA. By design, the corresponding plots for the FDFD and F0D0 lattices are indistinguishable from it.

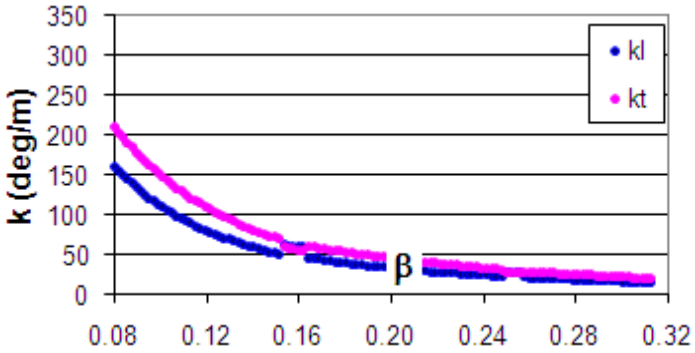

Figure 4. The real-estate phase advance for a 64-mA beam is the same in all 3 lattice configurations.

3. Acceptance

An important figure of merit for the focusing lattice in accelerators is its transverse acceptance. Acceptance is defined as the area in phase space within which charged particles can be transported without loss. Acceptance is usually referenced to the injection point of the linac and compared to the emittance of the injected beam. It gives an indication of the safety margin available to compensate for emittance growth, misalignments and beam steering. Acceptance is typically calculated using a multi-particle code in which large uniform arrays of particles in the 2 uncorrelated transverse phase planes are transformed through the linac without space charge. An ellipse is then fit to the initial coordinates of the survivors, the area of which is defined as the acceptance of the system.

We have initially used an analytic approach in evaluating acceptance for the three lattices as a function of β, the relativistic beam velocity. From the smoothed real-estate phase advance k_{0t} we can evaluate the area A of a matched beam ellipse in phase space whose average radius would just touch the drift tube bore (1).

$$A_{smoothed} = k_{0t}\, r_{bore}^2$$

In this smoothed case, since the bore radius r_{bore} is constant throughout the linac, the acceptance would just be proportional to $k_{0t,}$ which we have made essentially identical in all three lattices resulting no differences. Including the flutter factor ψ (2) more accurately reflects the reduction in the acceptance due to the betatron oscillation which is a strong function of the lattice configuration. In this case the acceptance is determined by the radius of a matched ellipse that would, at its bust, just touch the bore. We define $A_{0,n}$ as the normalized acceptance at zero current.

$$A_{0n} = k_{0t}\, r_{bore}^2/\psi\beta\gamma,$$

$$\psi = r_{max}/r_{min}$$

where r_{max} and r_{min} are the maximum and minimum size of a matched beam in a focusing and defocusing lens, and $\beta\gamma$ is the relativistic momentum.

Figure 5 shows the acceptance for the three lattices as a function of β. Because acceptance is considered a property of the accelerator and is independent of any beam properties, space charge effects are normally irrelevant. Using this technique, however, we can apply the phase advance corresponding to full beam current (64 mA) k_t to see the effective reduction in acceptance at full-tune depression.

The two 4-period lattices have similar zero-current acceptance throughout, but we see that the final value for the FDFD lattice is slightly larger because the flutter factor is smaller. In all cases the normalized acceptance steadily decreases and is finally defined by its value at

the exit of DTL. This implies that there may be a "bottleneck" in transmission at the end of the DTL where the energy is the highest, precisely where we don't want to lose beam. If we look at the acceptance corresponding to full beam current we see that it follows the character of the zero-current values in all cases.

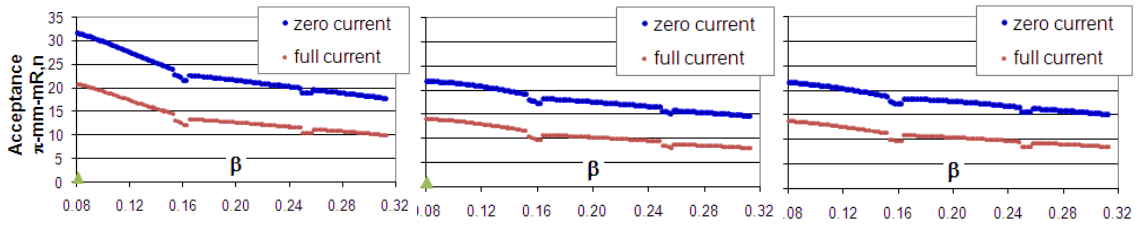

Figure 5. Normalized transverse acceptance as a function of β, a. FDFD, b. F0D0, c. FFDD.

The acceptance can be compared to the normalized emittance of our beam at the exit of the linac which, at full current is ~3π mm-mRad and contains ~99% of the particles. The acceptance and ratio of emittance to acceptance for each lattice is shown in Table 1. Because the FDFD lattice has the smallest ratio of emittance to acceptance it appears to be the most attractive choice.

Table 1 Acceptance for 3 Lattices

Lattice	$A_{0,n}$ π mm-mR	$\varepsilon/A_{0,n}$	A_n π mm-mR	ε/A_n
FDFD	17.70	17%	10.00	30%
F0D0	14.66	20%	8.16	37%
FFDD	15.11	20%	8.57	35%

To independently verify this technique of calculating acceptance we have transported an array of "pencil beams" through the DTL using the envelope code LTrace, without space charge. Figure 6 shows the initial coordinates of beamlets that did not touch the drift-tube bore as they were accelerated through tank 1 (red) and through all three tanks (blue) of the DTL with an FFDD quadrupole lattice. The area of ellipses fit to these initial coordinates agrees with the value derived analytically. We can confirm from these plots that the acceptance of the full linac is ~85% of that defined by tank one alone as indicated in figure 5c.

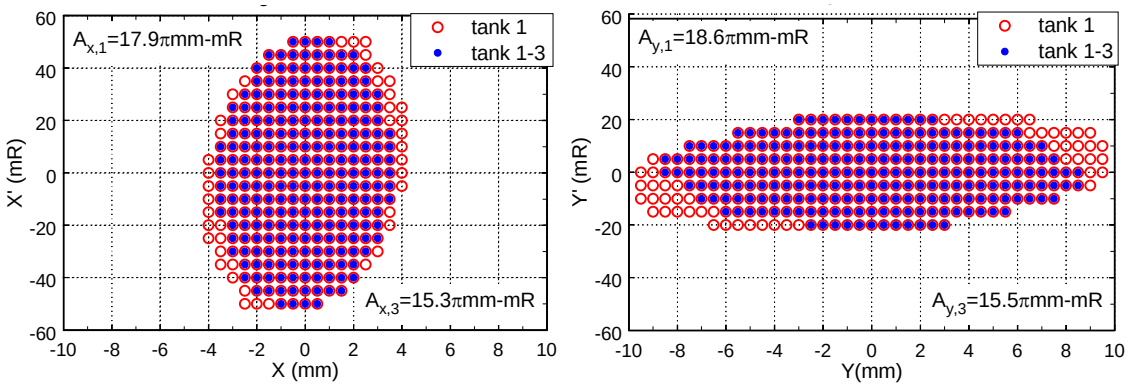

Figure 6. Transverse acceptance in an FFDD lattice.

4 Alignment errors

While the ratio of emittance to acceptance gives us a qualitative indication of the safety margin of the lattice design, it does not fully reflect the risk of beam loss in an imperfectly aligned machine. The quadrupoles in the DTL will be aligned within an absolute tolerance of ±0.3 mm. We expect that the alignment of individual quadrupoles will be distributed within a

Gaussian having a standard deviation of ±0.1 mm that is truncated at ±0.3 mm. As we will see below such a tolerance has the potential of causing an unacceptable deviation of the centroid of an unsteered beam from the axis.

Figure 7 shows the transverse profiles of a beam in an FFDD linac having a typical set of alignment errors that cause the edge of the beam to approach the drift-tube bore in tank 3. In this example, we can see that while there is plenty of clearance in tank 1, the final acceptance is defined by the effects of cumulative misalignments throughout the linac. Figure 8 shows the acceptance of this misaligned linac in which the filling factor is ~96%. Comparing these plots with those in figure 6 we see that the acceptance has been reduced by 20% and 30% in the x and y phase planes respectively. These plots indicate that to maximize the beam clearance throughout the linac we should inject the beam ~2.4 mm high and ~1.4 mm to the left. Figure 9 shows the improvement we can achieve by using pairs of steering magnets in the chopper line to correct the centroid trajectory of the injected beam.

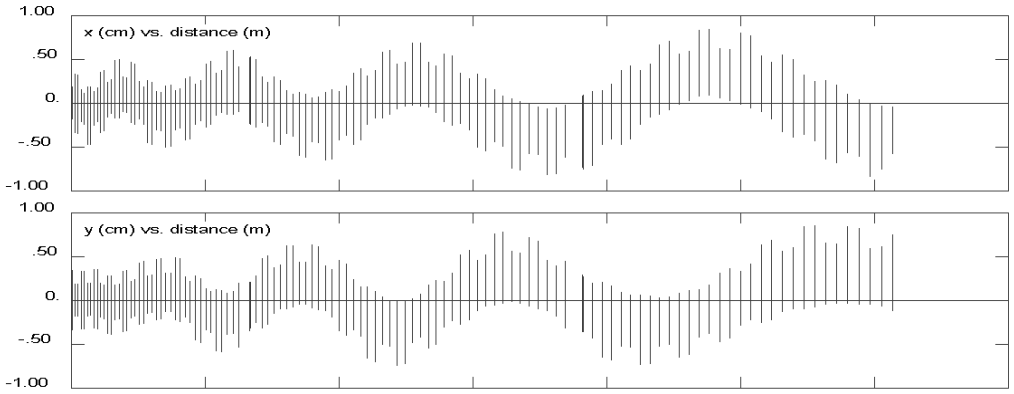

Figure 7. Transverse beam profiles in a misaligned linac.

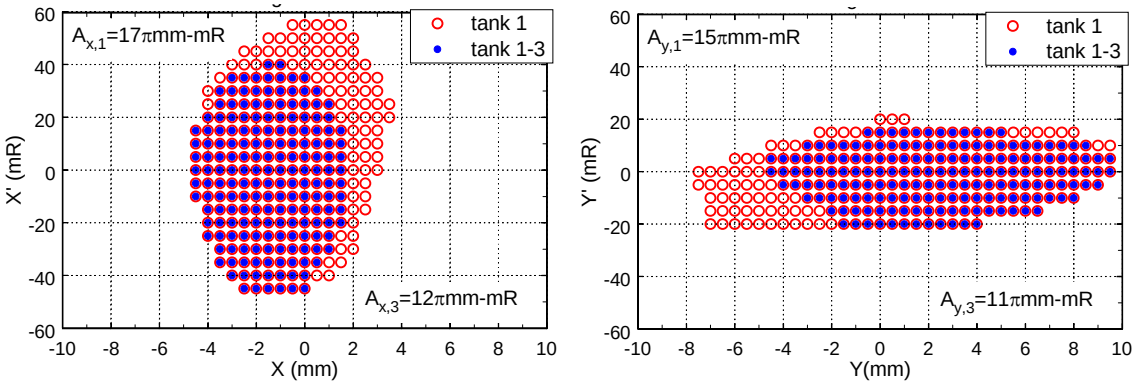

Figure 8. Reduced acceptance in an FFDD linac with alignment errors.

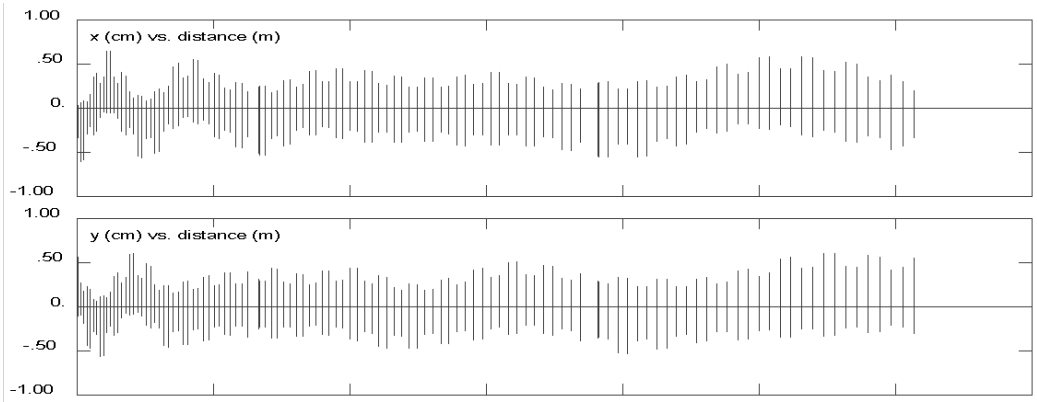

Figure 9. Transverse profiles in a misaligned linac for a beam injected off axis.

Identifying the centroid of the linac acceptance, which we can do empirically with a "pencil beam" and two pairs of steering magnets, is a good starting point for steering the beam through the linac.

The magenta curves in figures 10, 11, and 12 show the probability distributions for the deviation of the beam centroid from the linac axis for 1000 random sets of quadrupole alignment errors within the tolerance described above. In these plots we read on the ordinate the probability that the maximum centroid deviation will be less than or equal to the corresponding radial displacement on the abscissa. For example, in figure 10 we see that in the worst case scenario (100%), the centroid would become displaced by less than 10 mm at some point in the linac. With 90% probability it would be displaced no more than 7 mm. The expected displacement (50%) would be only 4.6 mm.

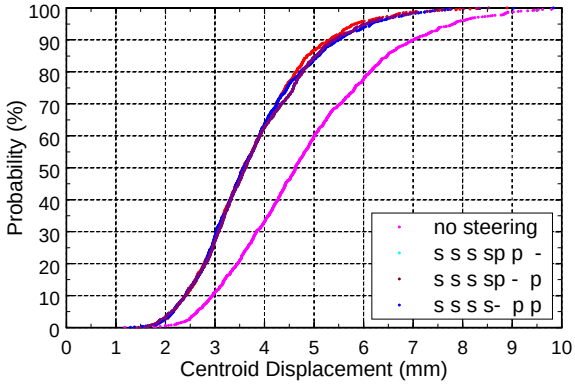

Figure 10. FDFD, Probability plot of beam centroid displacement with and without Minimum Steering.

In the F0D0 lattice worst case scenario, figure 11, we would not expect the maximum centroid excursion to exceed 6.5 mm. Likewise in the FFDD lattice, figure 12, we would not expect the centroid to deviate more than 6.5 mm. The "expected" value for the centroid deviation, corresponding to the 50th percentile, would be 4.6, 3.5, and 3.3 mm respectively for the three lattice configurations. So we can expect the centroid excursion to be ~40% larger in the FDFD lattice than in the FFDD lattice.

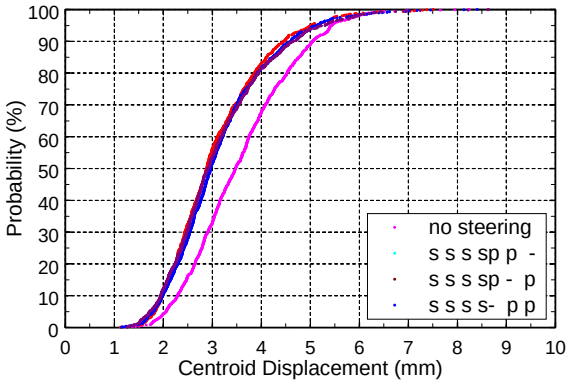

Figure 11. F0D0, Probability plot of beam centroid displacement with and without Minimum Steering.

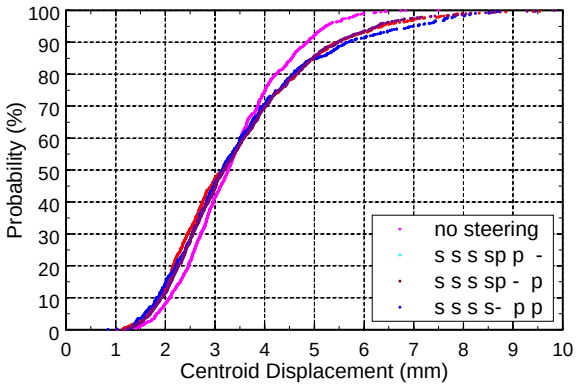

Figure 12. FFDD, Probability plot of beam centroid displacement with and without Minimum Steering.

In an attempt to mitigate the potential for beam loss due to alignment errors, the DTL design includes bipolar steering magnets in both transverse planes preceding each tank and beam position monitors (BPMs) following each tank. Figure 13 shows schematically the location of these correctors and diagnostics in Linac4.

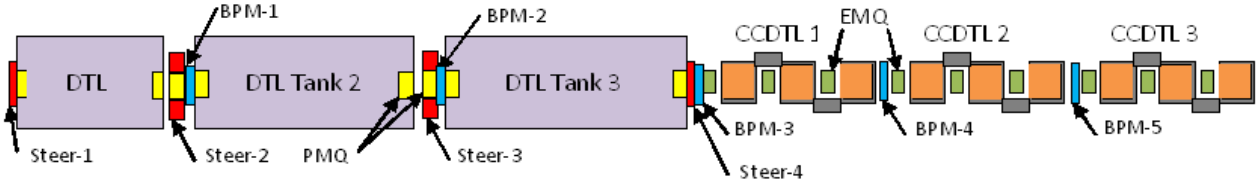

Figure 13. Locations of steering magnets and beam position monitors.

Our ultimate objective in correcting the beam trajectory is to minimize beam loss, particularly at high energies. Unfortunately, the limited number of diagnostics and correction elements does not allow us to steer an errant beam back onto the axis anywhere within the DTL. By steering the beam onto the axis at the BPMs we would only be guaranteeing that the beam crosses the axis at those locations which could result in large excursions between BPMs.

5. Minimum steering

We have investigated the application of a steering algorithm called "minimum steering" in which we use the 4 steering magnet pairs in the DTL to put the beam on axis as determined by a pair of BPMs located downstream of the DTL. In this algorithm we are seeking steering strengths to put the beam on axis at two BPMs while at the same time minimizing the sum of the squares of the steering strengths required. If the steering strengths are minimized then the beam oscillation amplitude is typically kept to a minimum. If not, then more steering would be required. By minimizing the sum of the squares of the deviation of the beam centroid from the axis at the BPMs, rather than insisting that it be precisely on axis, we can find solutions that minimize the amount of steering required while maximizing the colinearity of the beam with the machine axis. This approach typically results in minimizing the centroid excursions within the DTL, which is our primary goal.

So how well does minimum steering work in this application? It does not work very well. We tested this algorithm using three different pairs of BPMs following the DTL but found no combination that improved the algorithm's ability to minimize excursions. In the FDFD lattice minimum steering was able to correct the centroid excursion on average by only 1 mm as we see in figure 10. The multiple curves correspond to steering solutions using 3 different combinations of BPMs. Figure 11 shows that the algorithm reduced the expected deviation by

only ~ 0.5 mm in the F0D0 lattice while it only made things worse in the FFDD lattice, as we see in figure 12.

6. Reference Beam Size

Our steering studies are based on envelope equations in which we assume a beam which is equivalent to a one having a uniform particle distribution with an area equal to 5 times the rms value of the expected beam emittance. To make assertions about filling factors we need to make some assumptions about the size of the beam itself.

We start with an initial 100k-particle distribution that is monoenergetic, continuous in phase, and uniform in the matched 4-dimensional x, x', y, and y' hyperspace. We have transported this beam, using the multi-particle code Travel, from the ion source through the LEBT, RFQ and Chopper Line to the DTL entrance and then through the linac using a FDFD lattice. Figure 14 shows the transverse phase-space projections of this beam at the DTL entrance. The ellipses represent rms fits to the particle coordinates in x-x' and y-y'. In both planes the normalized rms emittance $\varepsilon_{rms,n} \approx 0.3\pi$ mm-mRad. The ellipses plotted in the figure have an area of 9 $\varepsilon_{rms,n}$ and enclose ~99% of the beam.

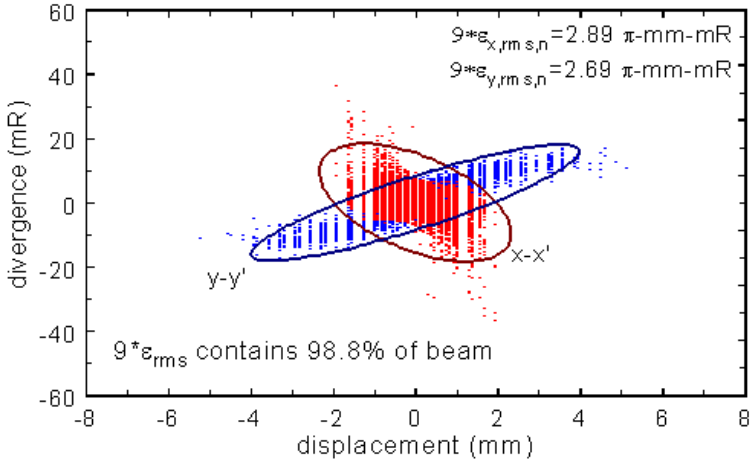

Figure 14. Transverse emittance projections at the DTL entrance.

Figures 15a and b show the horizontal and vertical phase-space projections of the beam as it exits the DTL having suffered only about 5% emittance growth. At the DTL exit ~98.5% of the beam is still contained within $9\varepsilon_{rms}$. Figure 16 shows the radial frequency distribution of the beam at the entrance and exit of the DTL. At the entrance, 99.8% of the beam is contained within 3σ radially which corresponds to $9\varepsilon_{rms}$. in phase-space area. Upon exiting the DTL, 99.95% of the beam is included within 3σ radially.

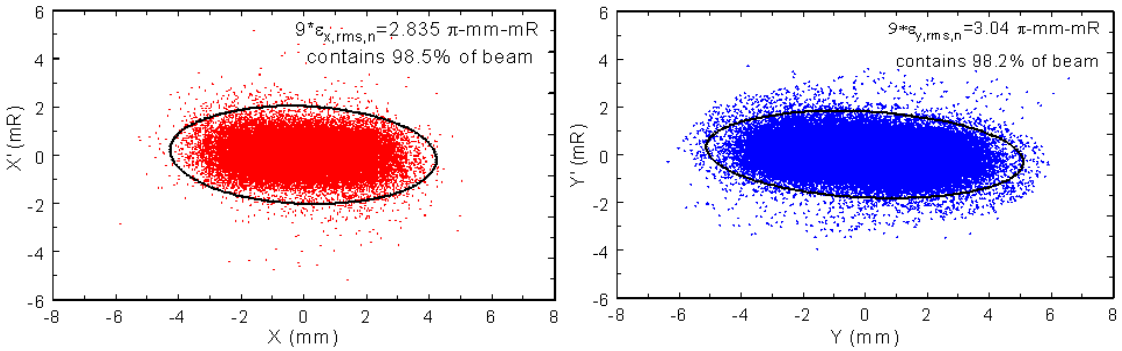

Figure 15. Horizontal (a) and vertical (b) emittance projections at DTL exit.

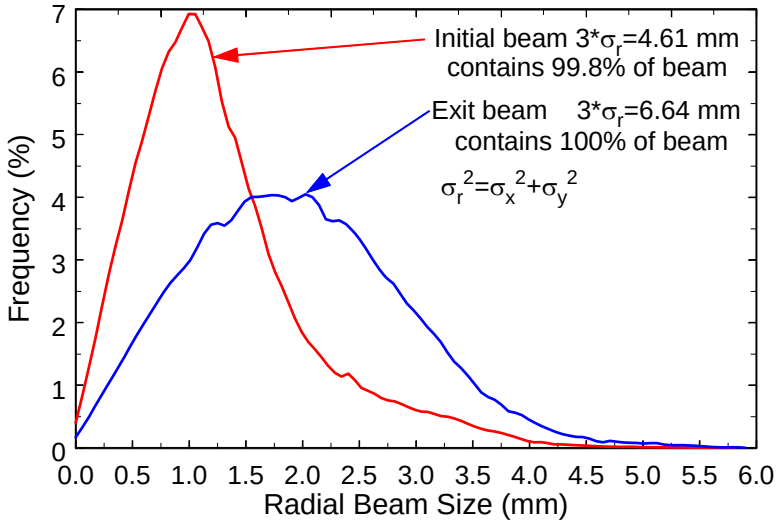

Figure 16. Radial particle distribution at DTL entrance and exit.

For the steering studies we have chosen to identify the "edge" of the beam to be at 3σ of its distribution in real space (x, y, and r) or 9σ in phase space (ε_x and ε_y) keeping in mind that as much as 1.5% of the beam could lie well outside of these values, as we see in figures 14 and 15. We define the filling factor as the fraction of the clear bore filled by the beam at 3σ of its radial distribution at its closest approach to the bore as it travels through the linac.

7. Intuitive steering

At many accelerator facilities the initial steering is carried out according to some sophisticated algorithm that derives partial derivatives experimentally and solves for the optimum steering solution. Following initial tune up, the operators typically "tweek" the steering intuitively to maximize transmission and minimize the prompt radiation. The "final" steering solution typically does not correspond to an axial beam as determined by the BPMS. We will refer to the subsequent steering as "intuitive steering."

We have investigated intuitive steering in Linac4 in which we use the 3 pairs (x and y) of steering magnets in the DTL to maximize beam transmission and minimize the maximum filling factor. Normally we consider the filling factor to be a figure of merit for a steering solution. In this scheme we are assuming that it is proportional to beam loss from the halo, which we hope to measure using beam-current transformers and radiation spill monitors, and so we use it as the dependent variable.

In this simple scheme we steer tank-by-tank. First, the horizontal corrector, located upstream of tank 1, is scanned to find the minimum filling factor (maximum transmission and minimum radiation) in tank 1. This is followed by scanning the vertical corrector to again find the minimum filling factor. This can be iterated if necessary or, if the steering space is skew or displaced, a two-dimensional scan may be necessary. We did not observe any local minima in the steering space. We proceeded to steer in the same way in tank 2 followed by tank 3.

How well does intuitive steering work? It actually works pretty well. The red curves in figures 17a, 18a and 19a show the probability distribution of filling factor for 1000 sets of quadrupole alignment errors within the tolerance described above. These curves correspond to the magenta curves in the probability plots of expected centroid deviation shown in figures 10, 11 and 12. Figure 17a shows that with 55% probability the beam will not intercept the drift-tube bore anywhere in the linac with FDFD focusing. With intuitive steering, limited to steering strengths of ±2 mT-m (blue curve) we can increase this to this to ~93%. Increasing

the range of the steering magnets to ±3 mT-m (magenta curve) only marginally improves the solution.

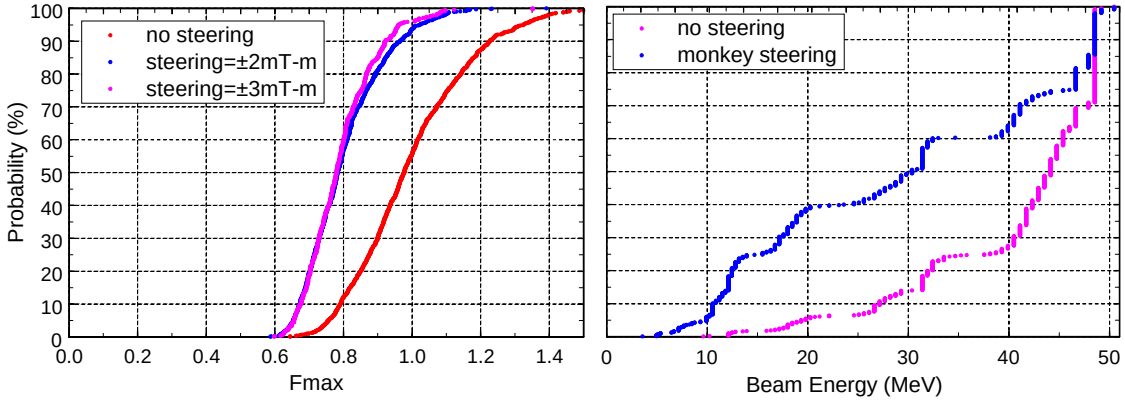

Figure 17. FDFD, Probability plot of a. maximum filling factor and b. beam energy at Fmax.

Figure 17b shows the expected energy at which the beam most closely approached the bore. The magenta curve shows the probability that, without any steering, the beam comes closest to the bore at or below the energy on the abscissa. In this FDFD lattice with a only a ~30% probability we would expect the closest approach to occur at an energy of less than 40 MeV. With steering the probability of beam spill becomes almost linear with energy, as shown by the blue curve. However, there would still be a 25% chance that any beam spill would occur at energies above 45 MeV.

Figure 18a shows that with an 65% probability the beam will not intercept the drift-tube bore anywhere in the linac with F0D0 focusing. With intuitive steering the probability increases to 95%. Figure 18b shows that without steering there is a large probability that any beam loss would occur at energies above 40 MeV. With steering the expected beam spill becomes linear with energy.

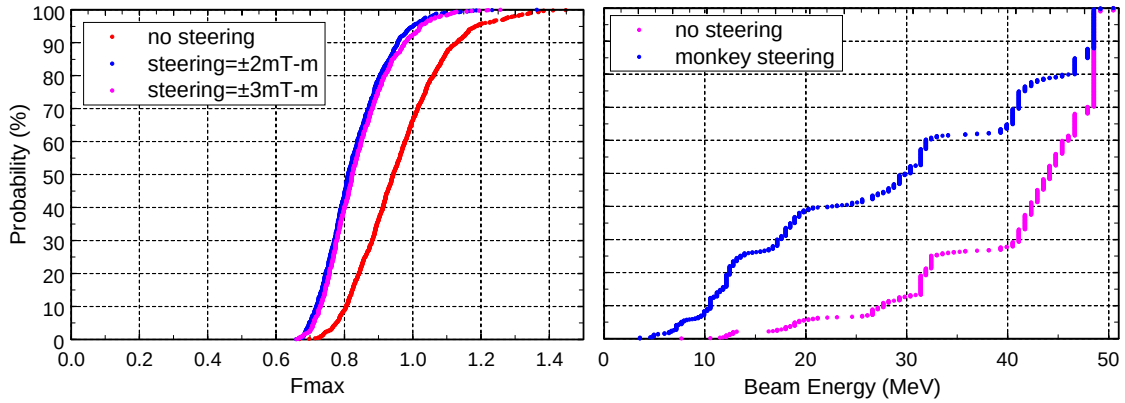

Figure 18. F0D0, Probability plot of a. maximum filling factor and b. beam energy at Fmax.

Figure 19 shows that with 85% probability the beam would not intercept the drift-tube bore anywhere in the linac with FFDD focusing. With intuitive steering we were able to increase that to 99% using steering strengths limited to ±2 mT-m. In fact, the expected filling factor (50th percentile) would be a little over 0.7. Figure 19b shows that steering would also reduce the expected maximum energy of lost particles from ~45 MeV to ~30 MeV.

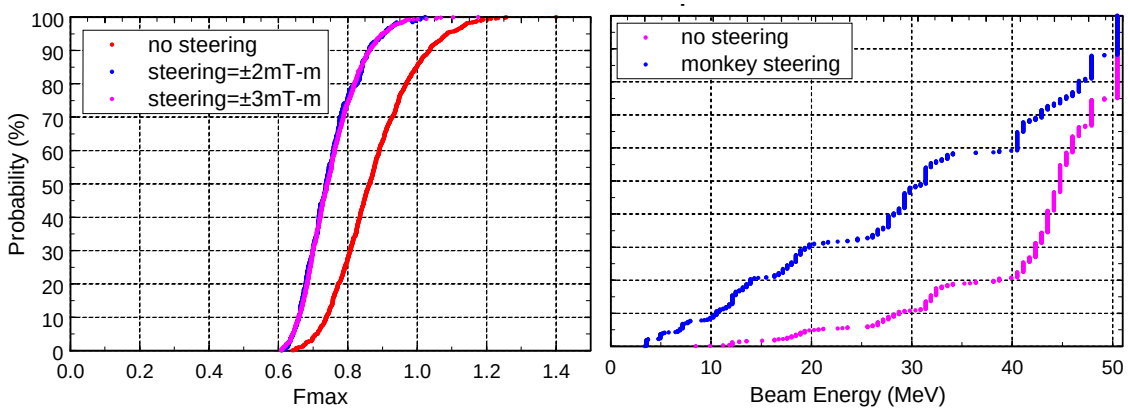

Figure 19. FFDD, Probability plot of a. maximum filling factor and b. beam energy at Fmax.

Figure 20 shows a frequency distribution of the steering strengths required in the 6 correctors for the 1000 steering solutions plotted in figure 19. These plots correspond to solutions in which we allowed the correctors to have a field of ±3 mT-m. In fact, as we can see in figure 19a, we can achieve the same performance with magnets limited to ±2 mT-m.

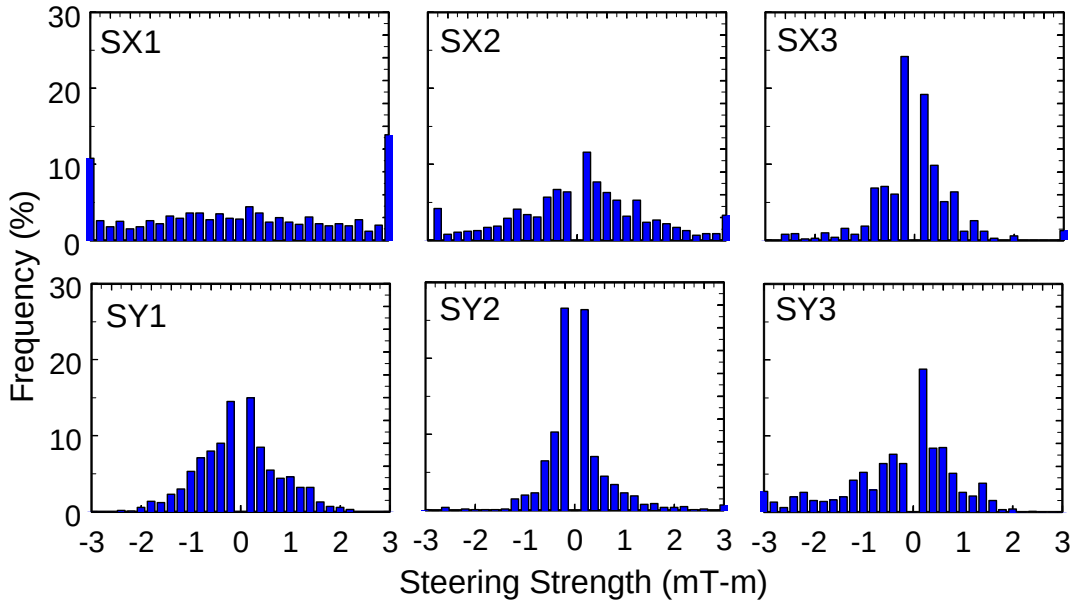

Figure 20. FFDD, Frequency of steering magnet requirements.

8 Conclusions

The objective of this study was to identify the best focusing lattice for the Linac4 DTL. Based on acceptance alone the FDFD lattice appears to be the most attractive. Based on statistical studies of the expected centroid excursion and filling factors we would eliminate FDFD as being the most sensitive to errors. Based on the minimum steering algorithm we cannot make any recommendation at all. With intuitive steering, however, it is clear that we can expect to minimize our risk of beam loss in the DTL with an FFDD lattice using realistic steering strengths and without relying on the limited number of BPMs available. While the F0D0 lattice is the cheapest and offers the option of including diagnostics in the empty drift tubes, it has, marginally, the worst performance of the three with steering included.

This study has illuminated another important point. Using the analytical approach to calculating the acceptance of the DTL we see in all cases that it decreases with increased energy creating a potential bottleneck at 50 MeV. This reduction in acceptance is reflected in

the expected loss energy for beam halo intercepting the bore. It is a result of the design procedure in which the longitudinal and transverse restoring forces are just balanced with the space-charge forces to avoid predicted resonances. We recommend that modifications to the design be investigated that would increase the effective acceptance at higher energies. There are at least two possibilities: 1, increase the transverse focusing at higher energy, and 2, increase the drift-tube bore in tanks 2 and 3.

References

1. Weiss, M. and Lapostolle. P. *Formulae and Procedures Usefull for the Design of Linear Accelerators.* Geneva, Switzerland : CERN-PS-2000-001 (DR). p35.

2**.** Wangler, T. *Principles of RF Linear Accelerators***.** John Wiley & Sons, Inc., 1998. p280.